Amorphous Alumina Films Efficiently Protect Ti6242S against Oxidation and Allow Operation above 600 °C

Diane Samélor, Loïc Baggetto, Raphaël Laloo, Viviane Turq, Thomas Duguet, Daniel Monceau, Constantin Vahlas

doi:10.4028/www.scientific.net/MSF.941.1846

Amorphous Alumina Films Efficiently Protect Ti6242S against Oxidation and Allow Operation above 600 °C

SAMELOR Diane[1,a], BAGGETTO Loïc[1,b], LALOO Raphaël[2,c], TURQ Viviane[2,d], DUGUET Thomas[1,e], MONCEAU Daniel[1,f] and VAHLAS Constantin[1,g*]

[1]CIRIMAT, Université de Toulouse
4, allée Emile Monso, BP-44362, 31030 Toulouse cedex 4, France

[2]CIRIMAT, Université de Toulouse
118 Route de Narbonne, 31062 Toulouse cedex 9, France

[a]diane.samelor@ensiacet.fr, [b]loic_baggetto@yahoo.fr, [c]laloo@chimie.ups-tlse.fr, [d]turq@chimie.ups-tlse.fr, [e]thomas.duguet@ensiacet.fr, [f]daniel.monceau@ensiacet.fr, [g*]constantin.vahlas@ensiacet.fr

Keywords: amorphous alumina; Ti6242; oxidation; barrier coating; chemical vapor deposition.

Abstract. The protection of the titanium based Ti6242S alloy against oxidation at moderate temperature is investigated, through the application on its surface of a 300 nm thick, amorphous alumina film. The latter is processed by metalorganic chemical vapor deposition at 500 °C from dimethyl aluminum isopropoxide. Upon oxidation at 600 °C for 5000 h, an interfacial zone is created between the alloy and the external protective layer, composed of unaffected alumina. In these conditions, the mass gain per unit area is eight times lower than that of the bare alloy, while the hardness of the alloy remains unaffected, revealing negligible oxygen ingress attributed to the efficiency of the protective coating. Finally, alumina coated samples show negligible mass change after 80 one-hour thermal cycles between 50 °C and 600 °C, showing excellent coating adherence on the Ti alloy.

Introduction

Implementation of lightweight titanium alloys in numerous key enabling technologies is hindered by their limited resistance to high temperature oxidation. This drawback is due to the rapid formation on the surface of titanium alloys in contact with the air, of a very stable, non-protective oxide layer, mainly composed of TiO_2. It is also due to the ingress of oxygen at interstitial position in the alpha phase of these alloys [1]. Indeed, the alpha hcp phase of Ti-alloys dissolves up to 33 at% of oxygen. Because of this very high concentration at the local equilibrium between the oxide and the metal, a diffusion flux of oxygen arises towards the bulk of the alloy. This diffusion generally affects a much thicker sub-surface zone than the thickness of the external oxide scale. The properties of this zone drastically change with regard to those of the bulk alloy: the cell parameter "c" of the hcp-Ti phase increases, the Young modulus and the hardness increase and the ductility decreases [2]. The consequence of these structural and functional modifications is the formation of surface cracks under tensile loading or under thermal cycling [3]. To face this problem, several commercial alloys, such as Ti-6Al-2Sn-4Zr-2Mo (wt%) (Ti-6242), or Ti-5.8Al-4Sn-3.5Zr-0.5Mo-0.7Nb-0.35Si-0.06C (IMI 834) have been developed specifically for higher temperature use. Indeed, they show a much better oxidation resistance than pure titanium [4]. Nonetheless, for these alloys as well, the oxygen affected zone can be large at high operating temperature, for example 40 μm after only 500 h at 593 °C, or more than 80 μm for the same duration at 649 °C [4].

Tuning of the alloy composition and microstructure, and coatings solutions have been tested to prevent oxygen ingress in titanium and Ti alloys and limit the external oxide scale at the same time. The authors' and other groups investigated the deposition of Al coatings which, in operating conditions yield a protective Al_2O_3 superficial layer [5, 6]. However, the rough morphology of the

Al films is deleterious to the efficiency of the protective layer [7, 8]. A more straightforward approach is to directly deposit Al_2O_3 coatings. This approach has been successfully tested,[9] especially with amorphous Al_2O_3 processed by metalorganic chemical vapor deposition, MOCVD [10, 11].

The present work subscribes to this approach, by taking a deeper insight, also closer to the aero turbine specifications. MOCVD of amorphous Al_2O_3 films is performed from aluminum di-methyl isopropoxide, DMAI [12]. We report mass gain data from long term isothermal oxidation experiments, which allow determining the oxidation kinetics and provide an overall image of the oxidation process, with a part of the oxygen mass gain related to the external oxide scale formation, and another important part coming from the oxygen ingress in the alloy [13]. We investigate the interfacial zone by Auger electron spectroscopy and we probe the oxygen enriched zone on cross sections of the material, by determining the microhardness profile from the surface to the bulk. Finally, we illustrate the capacity of the amorphous Al_2O_3 coatings to sustain typical operating conditions of the titanium parts in aero turbines by cyclic oxidation tests at 600 °C.

Materials and Methods

Deposition of amorphous Al_2O_3 films was performed from in a custom-made, horizontal, 25mm diameter, 300 mm length hot-wall reactor presented in details in [14]. In short, Ti6242S coupons are placed on a stainless steel holder in the center of the quartz tube where the temperature is uniform, with a total reaction pressure of 5 Torr and a temperature of 500 °C unless otherwise mentioned. DMAI (>99%, Air Liquide) is transported to the deposition area with a direct liquid injection (DLI) technology (Kemstream), following a protocol described in details in [12]. The protocol consists in preparing a 0.2 M solution of DMAI in anhydrous cyclohexane (99.5%, H_2O<10 ppm, Sigma–Aldrich) without any contact with the air. 50 standard cubic centimeters (sccm) of O_2 (99.9995%, Air Products) is added to the N_2 dilution gas (300-400 sccm). The oxidant is in large excess compared to DMAI.

In order to measure the oxidation kinetics of uncoated and coated Ti6242S at several temperatures in a single short run, a specific experiment was designed and performed with a high precision thermogravimetric apparatus (SETARAM TAG24s). The experiment consists in increasing step by step the temperature and continuously measuring the mass gain of the sample. Cyclic oxidation tests are performed with a TGA apparatus which allows thermal cycling with continuous recording of the mass [15]. The sensitivity on mass variation of the instrument is 0.1 µg, allowing for detection of tiny spallation events.

Surface morphology of the samples was evaluated with scanning electron microscopy (SEM) with a FEI HELIOS 600i instrument operated between 5 and 10 kV. Samples measured with SEM were fractured then covered by a thin layer of sputtered platinum to prevent charging effects during observation of their cross section. Scanning Auger microscopy (SAM) was performed using a Thermoelectron MICROLAB 350 apparatus to monitor local chemical composition. Samples surface was cleaned by Ar^+ sputtering (3 keV, 1.5 µA) prior to analysis. Auger mapping was performed in snapshot mode with a primary e-beam of 10 keV and the built-in drift compensation.

Nanoindentation tests were carried out on the cross-sectioned samples using an UltraNanoIndenter apparatus from CSM Instrument (Anton Paar) with a Berkovich diamond indenter. The load was gradually increased until a maximum value of 30 mN, at which the load was maintained for 15 s, and then reversed down to zero. The loading and unloading rate was 60 mN/min. Elastic modulus and hardness were calculated from the load vs. depth curves with the method proposed by Oliver & Pharr [16]. Indents were positioned on a diagonal line through the cross-sectioned sample from the top surface to the diffusion zone and to the substrate (every 5 or 10 µm).

Results and Discussion

Fig. 1 shows top view and cross sectional SEM micrographs taken in secondary electrons (SE) mode of a coated sample. The surface is smooth at the nanoscale, with typical roughness values of about 1.5 nm. At the µm scale, polishing traces remain visible after deposition, and are covered with a conformal Al_2O_3 film. We can also note the presence of few nodules on the surface, also composed of Al_2O_3 and attributed to gas phase decomposition of DMAI leading to solid particles deposition. All coatings are composed of pure, stoichiometric, amorphous Al_2O_3 as revealed by X-ray and electron diffraction, electron probe microanalysis, X-ray photoelectron spectroscopy and Rutherford backscattering spectroscopy [12, 17].

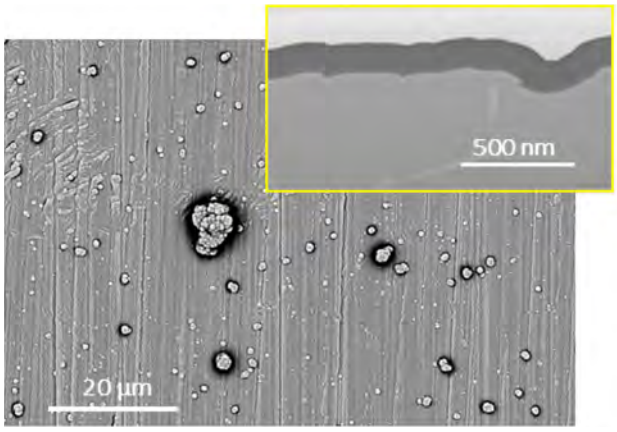

Fig. 1. SEM secondary electrons surface and cross section micrographs of the as processed, Al_2O_3 coated coupon.

Fig.2 presents surface SEM-SE micrographs of two samples after 5000 h of isothermal oxidation at 600°C. The left micrograph corresponds to the surface of bare Ti6242S. The whole surface is covered with thin, few-micrometers-long needles. This morphology corresponds to the well-known acicular rutile that forms when Ti6242S is exposed to oxidation treatments [13]. The right micrograph shows the surface of a TI6242S coupon coated with amorphous alumina. This Al_2O_3 surface presents less and thinner needles than those observed on the oxidized Ti6242S. In addition, we note the formation of a few excrescences on the surface.

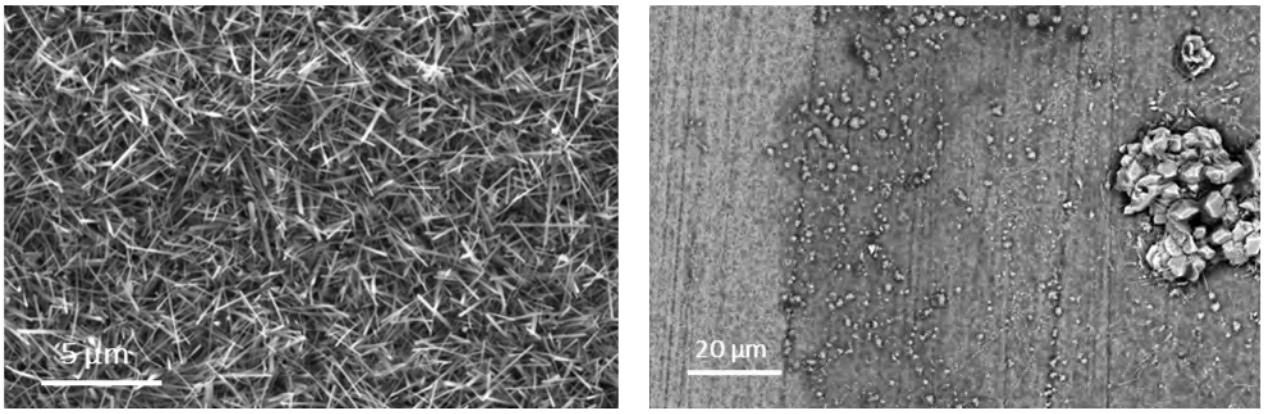

Fig. 2. Surface SEM-SE micrographs of two samples after 5000 h of isothermal oxidation at 600°C: bare Ti6242S (left), and coated coupon (right).

Fig.3 shows SEM images in backscattered electrons mode of cross-sections obtained by focused ion beam (FIB), and corresponding electron dispersive spectroscopy (EDS) maps of a bare Ti6242S alloy (Fig.3a-d) and a coated coupon (Fig.3e-h) after oxidation at 600 °C during 5000 h. The bare Ti6242S cross-section after oxidation (Fig.3a) can be divided into 3 layers. The top 1.6 µm-thick layer corresponds to the needles observed in Fig.2-left, with a great density of large open pores. The intermediate layer is 2 µm-thick, with a high density of small pores. The deepest region corresponds to the bulk part of the sample with the known microstructure of the alloy. The EDS mapping (fig.3a-d) reveals that a (Al, Ti) mixed oxide is formed on the top layer of the acicular rutile TiO_2 with a

clear preferential segregation of Al from the bulk to the free surface. In contrast, the intermediate layer mainly contains Ti and O. After oxidation of the coated coupon, its microstructure and chemical composition is strongly modified. Fig.3e shows the presence of pores in the vicinity of the initial alumina/Ti6242S interface. In this porous region, the Al_2O_3 coating has been replaced by a mixed Ti, O, Al layer. The thickness of the initial alumina protective film has been reduced by half at the end of the oxidation.

Fig.4 is composed of a SEM cross-section micrograph and of SAM maps of the coated coupon after oxidation. The maps reveal that the initial Al_2O_3 coating is now being replaced by a combination of two layers, a 250 nm thick (Ti, Al, O) and a 100 nm thin top (Al, O) one.

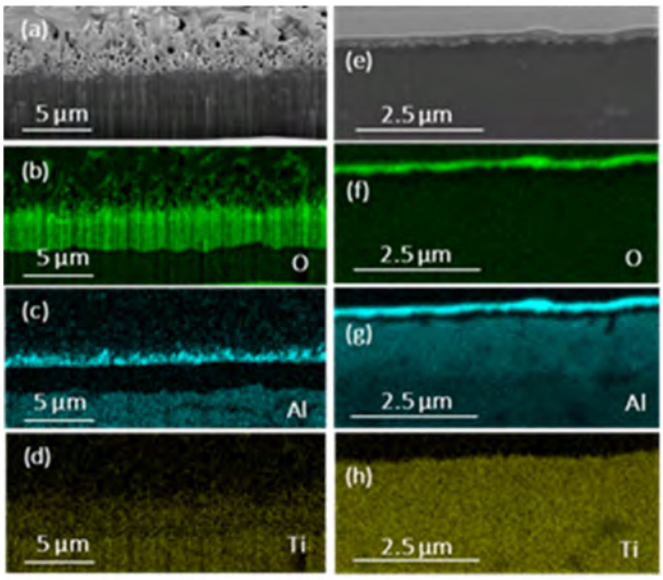

Fig. 3. SEM cross-sections and EDS mapping of O, Al, Ti elements of two samples after 5000 h of isothermal oxidation at 600°C: bare Ti6242S (a-d), and coated coupon (e-h).

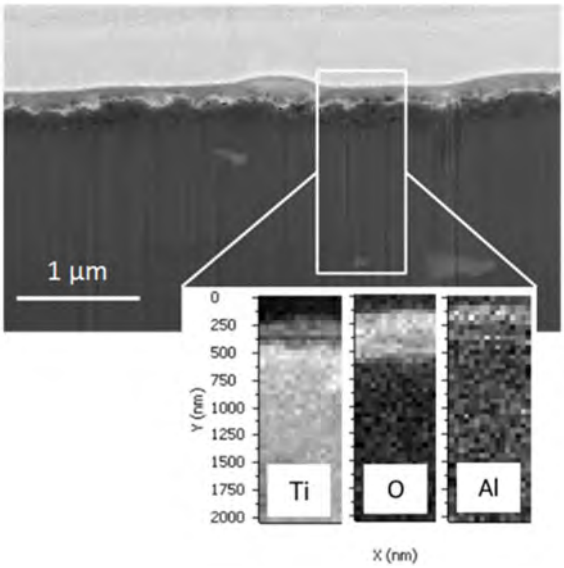

Fig. 4. FIB-SEM cross-section and Auger mapping of a coated sample after oxidation during 5000 h at 600°C.

Fig. 5 shows the results for the bare and coated Ti6242S coupons. The bare alloy and the coated coupon show mass gain of ca. 0.1 mg*cm^{-2} and 0.005 mg*cm^{-2}, respectively, at the end of the 700 °C plateau. Above this temperature mass gain for both samples accelerates, stronger for the bare alloy. The coated coupon is much more resistant than the uncoated one up to 700 °C.

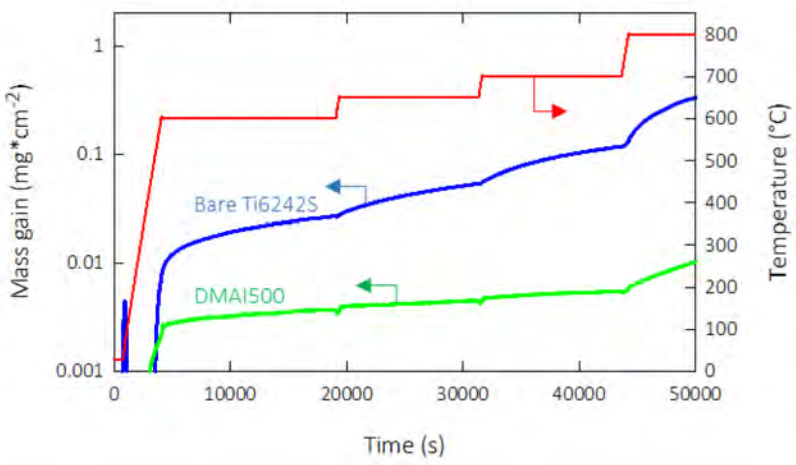

Fig. 5. Mass gain per unit area of bare and coated Ti6242S alloy as a function of time, for stepwise increasing annealing temperature (red curve).

TGA experiments were completed by long term oxidation annealing in laboratory air at 600 °C, which is closed to the maximum temperature of use of such alloys. Fig.6 presents the mass gain per unit area for bare and coated Ti6242S coupons as a function of the square root of annealing time for

5000 h. The figure shows limited weight gain of the coated Ti6242S compared to the bare one. The weight gain of the coated Ti6242S is 0.18 mg*cm^{-2} after 2300 h and 0.19 mg*cm^{-2} after 5000 h whereas the weight gain of bare Ti6242S is 0.624, 1.143 and 1.633 mg*cm^{-2} after 1000, 2500 and 5000 h, respectively. These results confirm the excellent oxidation protection conferred to Ti6242S by the ca. 300 nm thick amorphous Al_2O_3 films.

The behavior of the coated coupons was also evaluated under thermal cycling conditions. Indeed, in such conditions spallation of the ceramic coating on the metallic substrate may rapidly occurs resulting in limited durability of the material. The tests are performed with a TGA apparatus which allows thermal cycling with continuous recording of the mass [15]. The sensitivity on mass variation of the instrument is 0.1 µg, allowing for detection of tiny spallation events. 80 one hour cycles were performed between 50 °C and 600 °C, under flowing synthetic air. Fig. 7 presents the evolution of the mass gain per unit area of sample with a coating processed at 300 °C, and of the temperature variation as a function of time. No mass gain or mass loss could be detected for this sample at the microgram scale. Despite the fact that this test is rather short compared with the usual service periods in turbine applications, it is still a valuable indicator of the excellent adherence of the alumina layer and of the relatively low level of elastic strain energy in the system during thermal cycling.

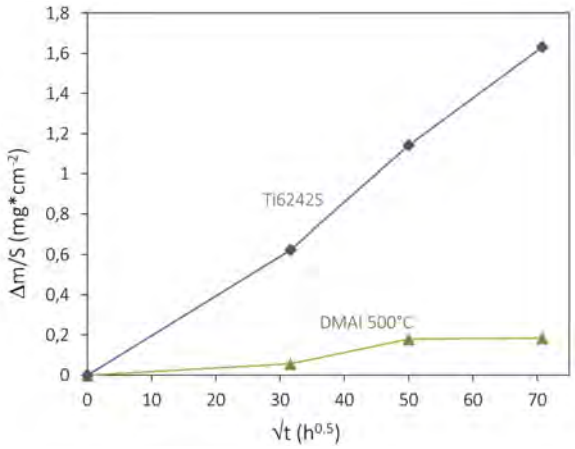

Fig. 6. Mass gain per unit area for bare and coated Ti6242S coupons as a function of the square root of annealing time at 600°C.

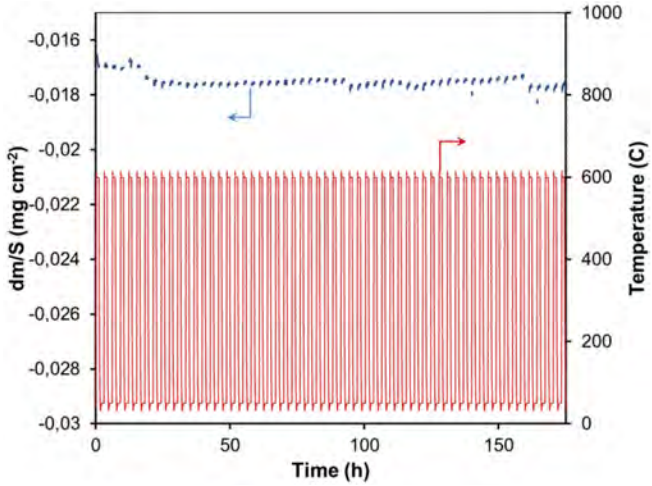

Fig. 7. Evolution of the mass gain per unit area of a sample coated at 300 °C, and of the temperature variation (cycling) as a function of time.

Fig. 8 shows the hardness (H) depth profile from top surface to the substrate as a function of penetration depth, for the bare Ti6242S and for the coated coupon after annealing at 600°C for 5000h. For the bare alloy, the hardness presents an increase from the bulk to the surface, reaching a peak value of 11.5 GPa, 10 µm beneath the surface whereas the hardness of the coated alloy shows a very limited increase. This increase of hardness for the bare alloy is explained by the oxygen diffusion zone. Both coupons present similar hardness values of about 4-5 GPa beyond 60 µm penetration depth until 140 µm below the surface. This result shows the good protection of the Al_2O_3 coating against oxygen ingress in Ti6242S alloy.

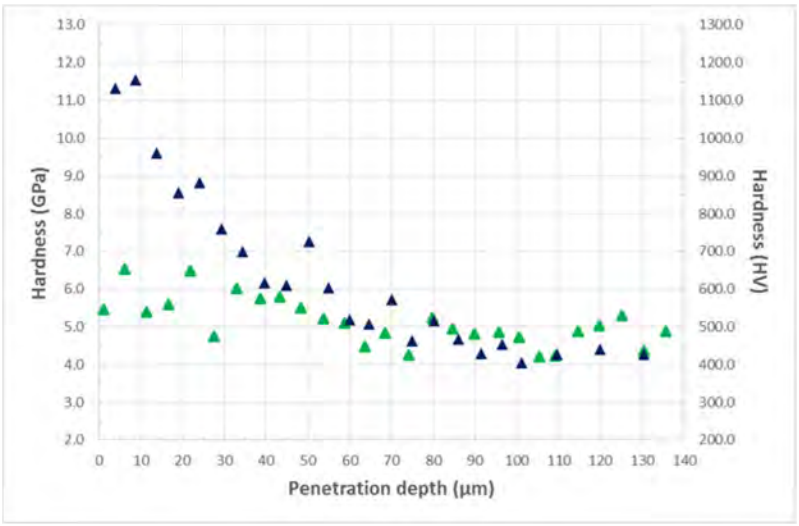

Fig. 8. Hardness depth profile as a function of penetration depth for the bare Ti6242S (blue) and for the coated coupon (green) after annealing at 600°C for 5000h.

Summary

The application by metalorganic chemical vapor deposition, of 300 nm thick amorphous alumina conformal coatings on the Ti6242S was performed at 500 °C using dimethyl aluminum isopropoxide. The aim is to investigate the resistance of the material against oxidation at high temperature and ultimately to extend the implementation of light titanium alloys in environments operating at temperatures at least as high as 600 °C. Isothermal oxidation tests performed at 600 °C reveal the formation of an interfacial layer between the alloy and the coating, composed of a complex titanium aluminum oxide. In these conditions, the mass gain per unit area is eight times lower than that of the bare alloy and the hardness of the alloy remains unaffected, revealing negligible oxygen ingress. Cyclic oxidation tests composed of 80 one hour cycles between 50 °C and 600 °C, under flowing synthetic air result in negligible mass gain and no coating spallation. These results confirm the efficiency of the protection of the alloy by the alumina coating. The MOCVD process is transferable and can be used for the surface treatment of parts of aeroturbines with complex shapes.

Acknowledgment

This work was financially supported by the STAE-RTRA foundation (Toulouse, France) under the RTRA-STAE/2014/P/VIMA/12 project grant.

References

[1] G. Lütjering, J.C. Williams, Titanium, Springer-Verlag, Berlin, Heidelberg, 2007.
[2] C. Leyens, M. Peters, Titanium and Titanium Alloys: Fundamentals and Applications, Wiley-VCH Verlag GmbH & Co. KGaA, Weinheim, 2003.
[3] A.L. Pilchak, W.J. Porter, R. John, Room temperature fracture processes of a near-alpha titanium alloy following elevated temperature exposure, Journal of Materials Science, 47 (2012) 7235-7253.
[4] K.S. McReynolds, S. Tamirisakandala, A Study on Alpha-Case Depth in Ti-6Al-2Sn-4Zr-2Mo, Metallurgical and Materials Transactions a-Physical Metallurgy and Materials Science, 42A (2011) 1732-1736.
[5] Q. Ru, S.J. Hu, Effects of Ti0.5Al0.5N coatings on the protecting against oxidation for titanium alloys, Rare Metals, 29 (2010) 154-161.
[6] M. Delmas, D. Poquillon, Y. Kihn, C. Vahlas, Al-Pt MOCVD coatings for the protection of Ti6242 alloy against oxidation at elevated temperature., Surf. Coat. Techn., 200 (2005) 1413-1417.

[7] M. Delmas, C. Vahlas, Microstructure of Metalorganic Chemical Vapor Deposited Aluminium Coatings on Ti6242 Alloy, J. Electrochem. Soc., 154 (2007) D538-D542.
[8] A.-L. Thomann, C. Vahlas, L. Aloui, D. Samélor, A. Caillard, N. Shaharil, R. Blanc, E. Millon, Conformity of Aluminum Thin Films Deposited onto Micro-Patterned Silicon Wafers by Pulsed Laser Deposition, Magnetron Sputtering, and CVD, Chem. Vap. Dep., 17 (2011) 366–374.
[9] Z.P. Jiang, X. Yang, Y.F. Liang, G.J. Hao, H. Zhang, J.P. Lin, Favorable deposition of gamma-Al2O3 coatings by cathode plasma electrolysis for high-temperature application of Ti-45Al-8.5Nb alloys, Surface & Coatings Technology, 333 (2018) 187-194.
[10] Y. Balcaen, N. Radutoiu, J. Alexis, J.D. Béguin, L. Lacroix, D. Samelor, C. Vahlas, Mechanical and barrier properties of MOCVD processed alumina coatings on TA6V titanium alloy, Surf. Coat. Techn., 206 (2011) 1684-1690.
[11] G. Boisier, M. Raciulete, D. Samélor, N. Pébère, A.N. Gleizes, C. Vahlas, Electrochemical behavior of chemical vapor deposited protective aluminium oxide coatings on Ti6242 titanium alloy, Electrochem. Sol. State Lett., 11 (2008) C55-C57.
[12] L. Baggetto, C. Charvillat, J. Esvan, Y. Thébault, D. Samélor, H. Vergnes, B. Caussat, A. Gleizes, C. Vahlas, A process-structure investigation of aluminum oxide and oxycarbide thin films prepared by direct liquid injection chemical vapor deposition of dimethylaluminum isopropoxide (DMAI), Chem. Vap. Dep., 21 (2015) 343-351.
[13] C. Dupressoire, A. Rouaix-Vande Put, P. Emile, C. Archambeau-Mirguet, R. Peraldi, D. Monceau, Effect of Nitrogen on the Kinetics of Oxide Scale Growth and of Oxygen Dissolution in the Ti6242S Titanium-Based Alloy, Oxidation of Metals, 87 (2017) 343-353.
[14] L. Baggetto, J. Esvan, C. Charvillat, D. Samélor, H. Vergnes, B. Caussat, A. Gleizes, C. Vahlas, Alumina thin films prepared by direct liquid injection chemical vapor deposition of dimethylaluminum isopropoxide: a process-structure investigation., Physica Status Solidi C, 12 (2015) 989-995.
[15] D. Monceau, D. Poquillon, Continuous thermogravimetry under cyclic conditions, Oxidation of Metals, 61 (2004) 143-163.
[16] W.C. Oliver, G.M. Pharr, An improved technique for determining hardness and elastic-modulus using load and displacement sensing indentation experiments., J. Mater. Res., 7 (1992) 1564-1583.
[17] L. Baggetto, C. Charvillat, Y. Thébault, J. Esvan, M.C. Lafont, E. Scheid, G.M. Veith, C. Vahlas, Amorphous alumina thin films deposited on titanium: Interfacial chemistry and thermal oxidation barrier properties, Phys. Stat. Sol. A, 213 (2016) 470–480.